

Top-quark pair production in heavy-ion collisions



Patrycja Potępa

Petr Baroň,
Iwona Grabowska-Bołd,
Jiří Kvita, Santu Mondal,
Yuriy Volkotrub

JOHANNES GUTENBERG
UNIVERSITÄT MAINZ



Outline

1 Motivation

2 Proton and nuclear PDFs

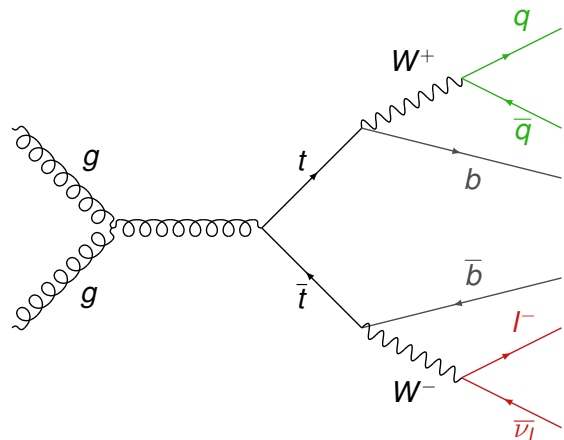
3 Reference measurements

4 Measurement of $t\bar{t}$ in $p+\text{Pb}$ collisions

5 Prospects of $t\bar{t}$ in $\text{Pb}+\text{Pb}$

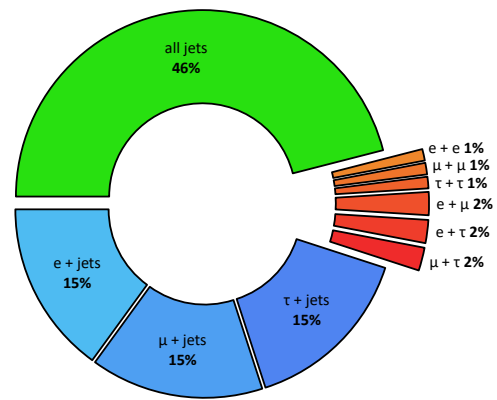
$t\bar{t}$ production

- ❖ Top quark is the heaviest elementary particle (175 GeV) and it decays before hadronisation.
- ❖ Top quark pair ($t\bar{t}$) is produced mainly via gluon fusion.
- ❖ Single top production has a lower cross section compared to $t\bar{t}$.
- ❖ $t\bar{t}$ process is sensitive to gluon parton distribution functions (PDFs).
- ❖ The final state consists of leptons and jets including two b-jets.



$t\bar{t}$ decay channels

- ❖ The $t\bar{t}$ cross section is measured in **$\ell+{\text jets}$** and **dilepton** channels in $p+{\text Pb}$ collisions in ATLAS ([ATLAS-CONF-2023-063](#)).
- ❖ The first measurement using the **dilepton channel** in $p+{\text Pb}$ collisions.
- ❖ A measurement in $p+{\text Pb}$ collisions using the **$\ell+{\text jets} \text{ channel}$** has been reported by CMS ([PRL 119, 242001 \(2017\)](#)).
- ❖ An evidence in ${\text Pb}+{\text Pb}$ collisions using the **dilepton channel** has been reported by CMS ([PRL 125 \(2020\), 222001](#)).



$\ell + {\text jets} : \quad t\bar{t} \rightarrow W b W \bar{b} \rightarrow \ell \nu_\ell b q \bar{q}' \bar{b}$
dilepton : $t\bar{t} \rightarrow W b W \bar{b} \rightarrow \ell \nu_\ell b \bar{\nu}_\ell \bar{b}$

Proton PDFs

❖ **Global analysis** - a multi-experiment-multi-observable fit

❖ Fixed-target DIS and DY

- deep inelastic scattering (DIS) and Drell–Yan (DY) processes,
- important in setting the large- x quark distributions.

❖ HERA DIS

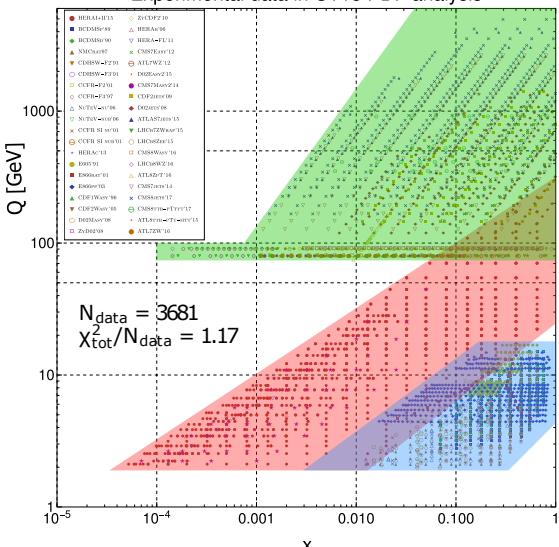
- access to a large x , Q^2 range.

❖ Hadron colliders

- access to new processes: W^\pm , Z , jets, $t\bar{t}$.

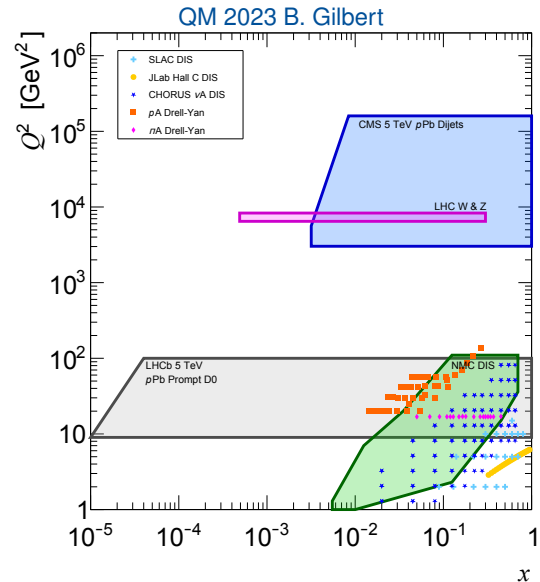
PRD 103, 014013

Experimental data in CT18 PDF analysis



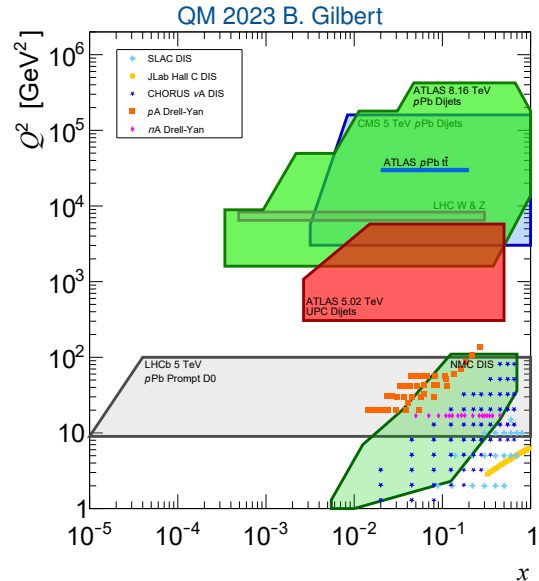
Nuclear PDFs

- ❖ World data constraining nuclear Parton Distribution Functions (nPDFs) shown on the (x, Q^2) plane.
- ❖ The kinematic coverage of experimental data has expanded massively with contributions from the LHC.
- ❖ Gaps still remain in the data determining nPDFs, leaving large stretches of phase space unconstrained.



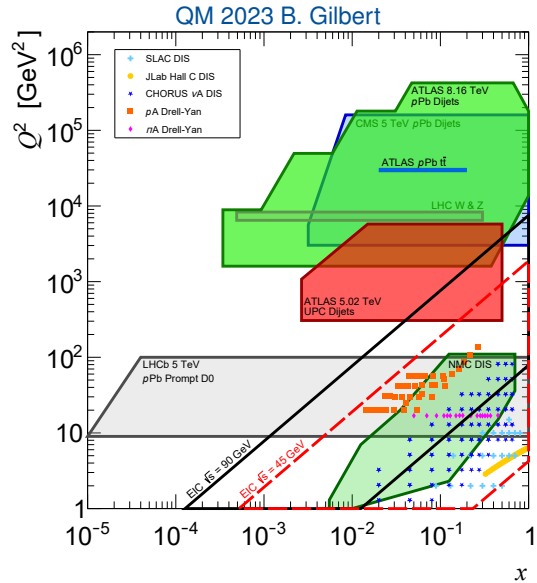
Nuclear PDFs

- ❖ Recent **ATLAS** measurements will help to constrain a large phase-space region.
- ❖ **UPC dijets 5.02 TeV**
 - ATLAS-CONF-2022-021
- ❖ **dijets 8.16 TeV $p+Pb$**
 - arXiv:2309.00033
- ❖ **$t\bar{t}$ 8.16 TeV $p+Pb$**
 - ATLAS-CONF-2023-063



Nuclear PDFs

- ❖ **Electron-Ion Collider (EIC)** will help to cover the gap on the (x, Q^2) plane.
- ❖ The project is years away, with estimated early completion in 2032.
- ❖ Recent ATLAS dijet results are closely related to the early physics goals of the EIC.



nPDF global fits

| nPDF | KSASG20 | nCTEQ15HQ | TUJU21 | EPPS21 | nNNPDF3.0 |
|-----------------------------------|------------------------|-----------------------|--------------------------|----------------------|-------------------------|
| | PRD 104, 034010 (2021) | PRD 105 (2022) 114043 | PRD 105 9 (2022), 094031 | EPJ C 82, 413 (2022) | arXiv:2201.12363 (2022) |
| Order in α_s | NLO & NNLO | NLO | NLO & NNLO | NLO | NLO |
| Free parameters | 9 | 19 | 16 | 24 | 256 |
| Independent flavours | 3 | 5 | 4 | 6 | 6 |
| Free-proton PDFs | CT18 | ~CTEQ6M | TUJU own fit | CT18A | ~NNPDF4.0 |
| Data points | 4353 | 940 | 2410 | 2077 | 2188 |
| ℓA NC DIS | ✓ | ✓ | ✓ | ✓ | ✓ |
| νA CC DIS | ✓ | | ✓ | ✓ | ✓ |
| $p A$ DY | ✓ | ✓ | | ✓ | ✓ |
| πA DY | | | | ✓ | |
| RHIC dAu π^0, π^\pm | | ✓ | | ✓ | |
| LHC pPb π^0, π^\pm, K^\pm | | ✓ | | | |
| LHC $p+Pb$ dijets | | | | ✓ | ✓ |
| LHC $p+Pb$ D^0 | | | | ✓ | ✓ |
| LHC $p+Pb$ W, Z | | ✓ | ✓ | ✓ | ✓ |
| LHC $p+Pb$ γ | | | | | ✓ |

nPDF global fits

| nPDF | KSASG20 | nCTEQ15HQ | TUJU21 | EPPS21 | nNNPDF3.0 |
|---------------------------------|------------------------|-----------------------|--------------------------|----------------------|-------------------------|
| | PRD 104, 034010 (2021) | PRD 105 (2022) 114043 | PRD 105 9 (2022), 094031 | EPJ C 82, 413 (2022) | arXiv:2201.12363 (2022) |
| Order in α_s | NLO & NNLO | NLO | NLO & NNLO | NLO | NLO |
| Free parameters | 9 | 19 | 16 | 24 | 256 |
| Independent flavours | 3 | 5 | 4 | 6 | 6 |
| Free-proton PDFs | CT18 | ~CTEQ6M | TUJU own fit | CT18A | ~NNPDF4.0 |
| Data points | 4353 | 940 | 2410 | 2077 | 2188 |
| ℓA NC DIS | ✓ | ✓ | ✓ | ✓ | ✓ |
| νA CC DIS | ✓ | | ✓ | ✓ | ✓ |
| $p A$ DY | ✓ | ✓ | | ✓ | ✓ |
| πA DY | | | | ✓ | |
| RHIC dAu π^0, π^\pm | | ✓ | | ✓ | |
| LHC pPb π^0, π^\pm, K^\pm | | ✓ | | | |
| LHC $p+Pb$ dijets | | | | ✓ | ✓ |
| LHC $p+Pb$ D^0 | | | | ✓ | ✓ |
| LHC $p+Pb$ W, Z | | ✓ | ✓ | ✓ | ✓ |
| LHC $p+Pb$ γ | | | | | ✓ |

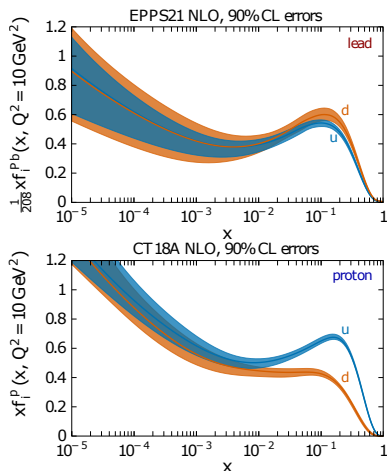
- ❖ Four nPDF sets include LHC data.

nPDF global fits

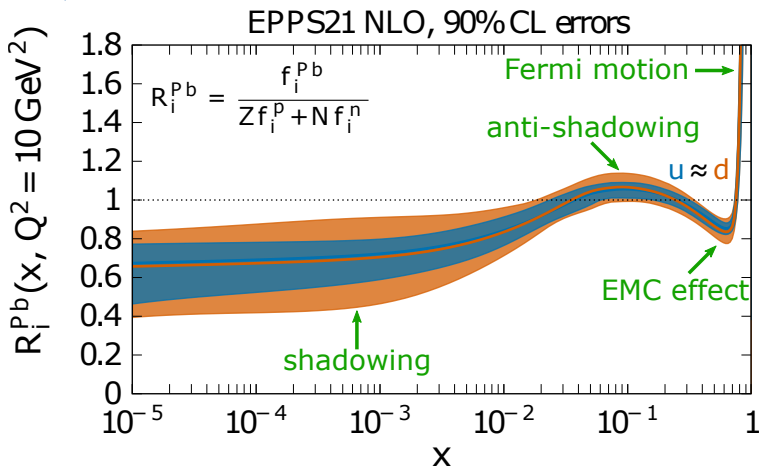
| nPDF | KSASG20 PRD 104, 034010 (2021) | nCTEQ15HQ PRD 105 (2022) 114043 | TUJU21 PRD 105 9 (2022), 094031 | EPPS21 EPJ C 82, 413 (2022) | nNNPDF3.0 arXiv:2201.12363 (2022) |
|-----------------------------------|-----------------------------------|------------------------------------|------------------------------------|--------------------------------|--------------------------------------|
| Order in α_s | NLO & NNLO | NLO | NLO & NNLO | NLO | NLO |
| Free parameters | 9 | 19 | 16 | 24 | 256 |
| Independent flavours | 3 | 5 | 4 | 6 | 6 |
| Free-proton PDFs | CT18 | ~CTEQ6M | TUJU own fit | CT18A | ~NNPDF4.0 |
| Data points | 4353 | 940 | 2410 | 2077 | 2188 |
| ℓA NC DIS | ✓ | ✓ | ✓ | ✓ | ✓ |
| νA CC DIS | ✓ | | ✓ | ✓ | ✓ |
| $p A$ DY | ✓ | ✓ | | ✓ | ✓ |
| πA DY | | | | ✓ | |
| RHIC dAu π^0, π^\pm | | ✓ | | ✓ | |
| LHC pPb π^0, π^\pm, K^\pm | | ✓ | | | |
| LHC $p+Pb$ dijets | | | | ✓ | ✓ |
| LHC $p+Pb$ D^0 | | | | ✓ | ✓ |
| LHC $p+Pb$ W, Z | | ✓ | ✓ | ✓ | ✓ |
| LHC $p+Pb$ γ | | | | | ✓ |

- ❖ KSASG20 and TUJU21 provide NNLO calculations.

Quark PDFs

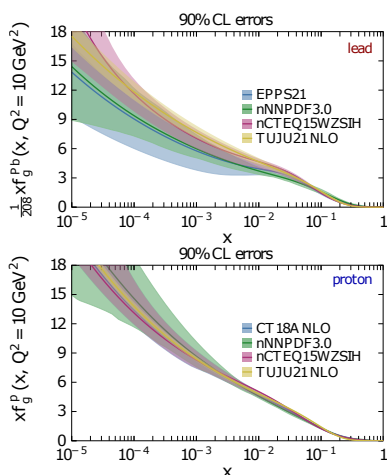


QM 2022 P. Paakkinen

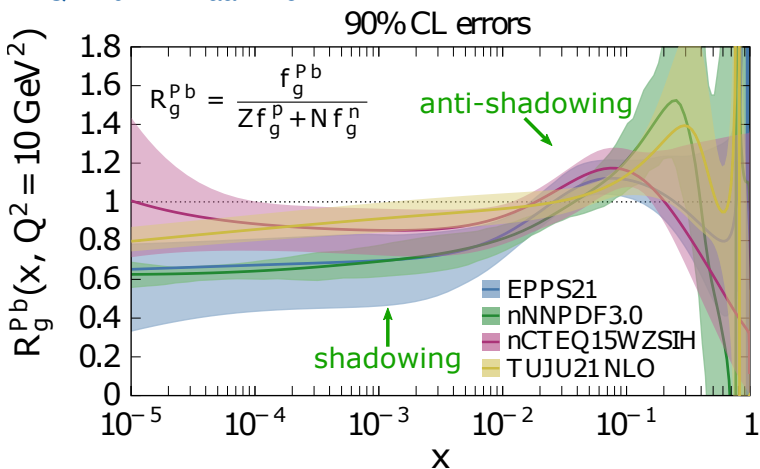


- ❖ EPPS21 nuclear modifications of bound protons in lead R_i^{Pb} at the initial scale $Q^2 = 10 \text{ GeV}^2$.
- ❖ Similar results for up and down quarks $u \approx d$.

Gluon PDFs



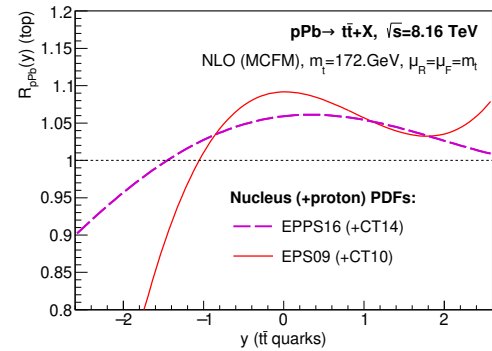
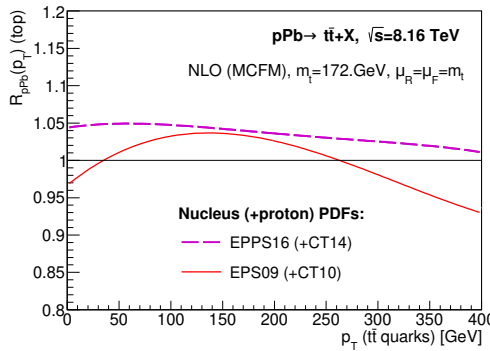
QM 2022 P. Paakkinen



- ❖ Nuclear modifications of bound protons in lead R_g^{Pb} for gluons with different nPDFs.
- ❖ Large errors and discrepancies between different nPDFs at high Bjorken- x values.

Top-quark probes

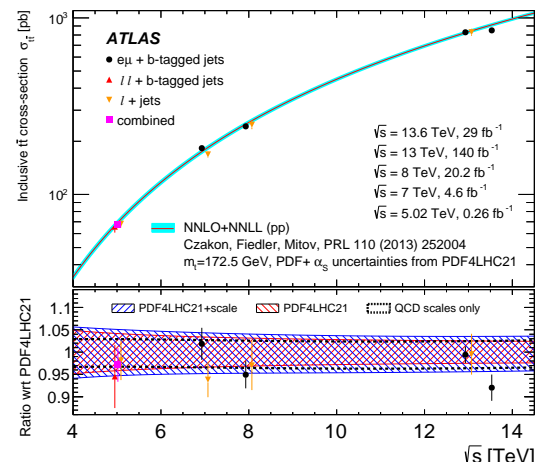
- ❖ Top quarks provide novel probes of nuclear modifications to nPDFs at high Bjorken-x values ([PRD 93, 014026 \(2016\)](#)).
- ❖ Nuclear modification factor ($R_{p\text{Pb}}$) prediction has been reported in [arXiv:1908.11534](#) as a function of $t\bar{t}$ pair p_T (left) and y (right).



ATLAS pp measurements

- ❖ ATLAS provides $t\bar{t}$ cross-section measurements in a wide centre-of-mass energy range.
- ❖ Measurements were done at 5 centre-of-mass energies:
 - 5.02 TeV
 - 7 TeV
 - 8 TeV
 - 13 TeV
 - 13.6 TeV
- ❖ Results are in agreement with theory predictions using the PDF4LHC21 PDF set.

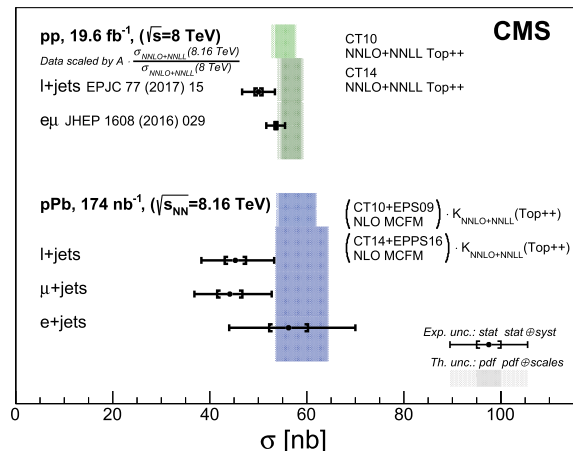
PLB 848 (2024) 138376



CMS $p+Pb$ measurement

- ❖ First observation of top-quark production in proton-nucleus collisions by the CMS.
- ❖ Total integrated luminosity of 174 nb^{-1} .
- ❖ Measurement done in $\ell+\text{jets}$ channel using a fit to invariant mass distributions of $t \rightarrow jj'b$ candidates.
- ❖ Combined cross section:
 $\sigma_{t\bar{t}} = 45 \pm 8 \text{ nb}$.
- ❖ Relative systematic uncertainty of 18%.

PRL 119, 242001 (2017)



ATLAS and CMS pp 7 and 8 TeV measurement

- ❖ The most precise $t\bar{t}$ cross-section measurement at 8 TeV scale.

JHEP 07 (2023) 213

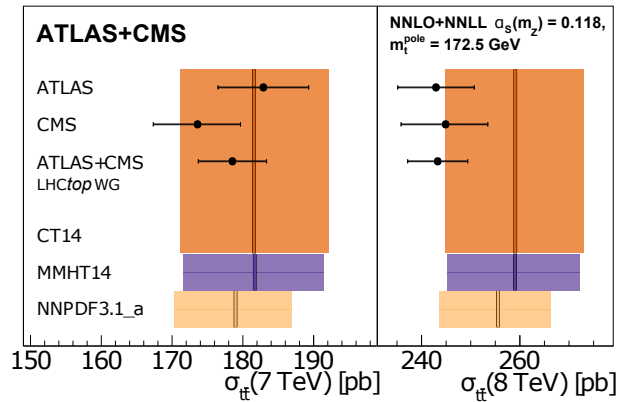
- ❖ Two measurements of the $t\bar{t}$ production in the $e\mu$ channel

ATLAS: EPJ C 74 (2014) 3109,
CMS: JHEP 08 (2016) 029.

- ❖ Measured cross section

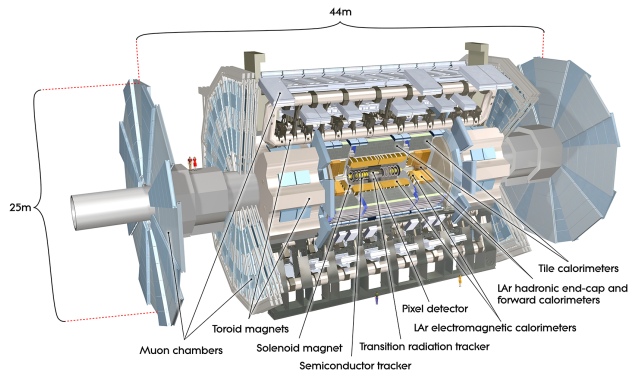
7 TeV: $\sigma_{t\bar{t}} = 178.5 \pm 4.7$ pb,
8 TeV: $\sigma_{t\bar{t}} = 243.3^{+6.0}_{-5.9}$ pb.

- ❖ $pp \sigma_{t\bar{t}}$ scaled by lead mass number A and extrapolated to 8.16 TeV can be compared to p+Pb $\sigma_{t\bar{t}}$.



ATLAS detector

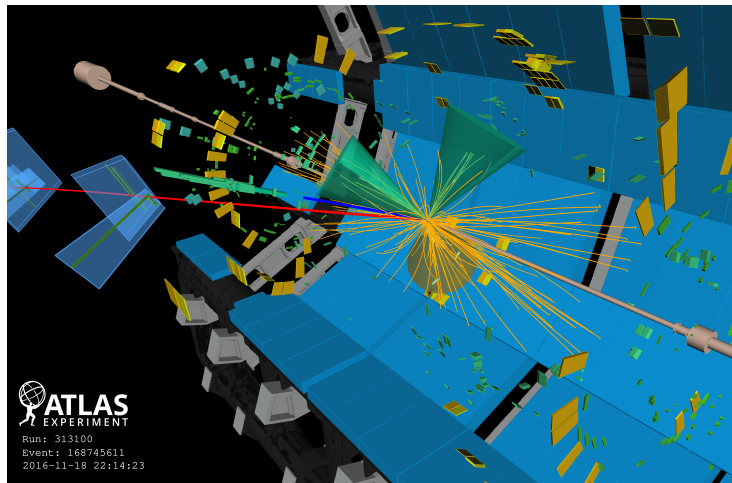
- ❖ A Toroidal LHC ApparatuS (ATLAS) is the largest, multi-purpose particle detector at the LHC.
- ❖ Three main systems are used in reconstruction:
 - inner detector,
 - calorimeter system,
 - muon spectrometer.
- ❖ The $t\bar{t}$ analysis uses reconstructed electrons, muons, jets, b -jets and missing energy.



Overview of the ATLAS detector.

$p+Pb$ data in ATLAS

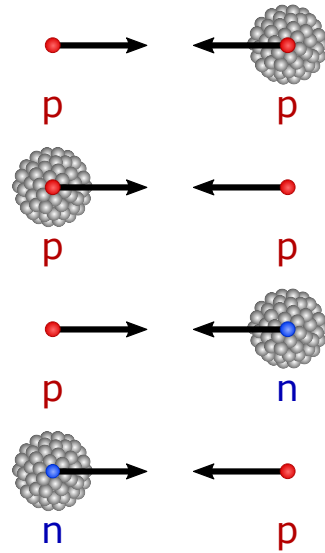
- ❖ $p+Pb$ data at $\sqrt{s_{NN}} = 8.16$ TeV collected in 2016 by ATLAS.
- ❖ The luminosity of **165 nb⁻¹**, split into **57 nb⁻¹** ($p+Pb$) and **108 nb⁻¹** ($Pb+Pb$).
- ❖ Final luminosity calibration with a relative uncertainty of **2.4%**.



Event display of a $p+Pb$ collision containing a $t\bar{t}$ candidate.

MC simulation

- ❖ MC samples produced using **Powheg+Pythia 8** and **Sherpa** generators.
- ❖ **Two isospin configurations:**
proton-proton (pp), proton-neutron (pn).
- ❖ **Two beam configurations:**
proton-lead (p+Pb), lead-proton (Pb+p).
- ❖ Events embedded into real p+Pb data forming **data overlay** samples.
- ❖ **Signal:** $t\bar{t}$,
Background: tW (single top), W , Z , diboson.



Event selection

$\ell + \text{jets}$

$e + \text{jets}$

- 1 electron,
- 0 muons,
- at least 4 jets.

$\mu + \text{jets}$

- 1 muon,
- 0 electrons,
- at least 4 jets.

Dilepton

ee

- 2 electrons,
- 0 muons,
- opposite sign leptons,
- $m_{\ell\ell} > 45 \text{ GeV}$ and $m_{\ell\ell} \notin (80 - 100) \text{ GeV}$,
- at least 2 jets.

$\mu\mu$

- 2 muons,
- 0 electrons,
- opposite sign leptons,
- $m_{\ell\ell} > 45 \text{ GeV}$ and $m_{\ell\ell} \notin (80 - 100) \text{ GeV}$,
- at least 2 jets.

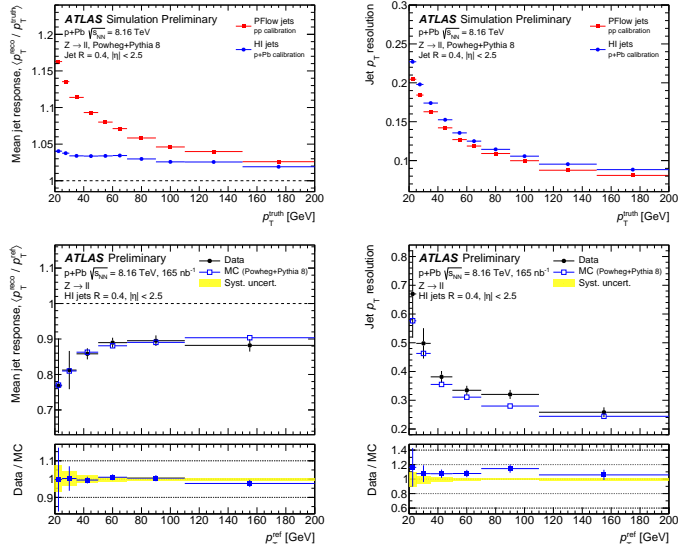
$e\mu$

- 1 electron,
- 1 muon,
- opposite sign leptons,
- $m_{\ell\ell} > 15 \text{ GeV}$,
- at least 2 jets.

Jet reconstruction

- ❖ Jets are required to have $p_T > 20 \text{ GeV}$ and $|\eta| < 2.5$.
- ❖ Jets are reconstructed using the anti- k_t algorithm with jet radius of $R = 0.4$.
- ❖ Two jet definitions are used
 - **heavy-ion (HI)** - dedicated for Pb+Pb collisions including underlying event correction,
 - **particle-flow (PF)** - standard jet definition with available b -quark tagging.

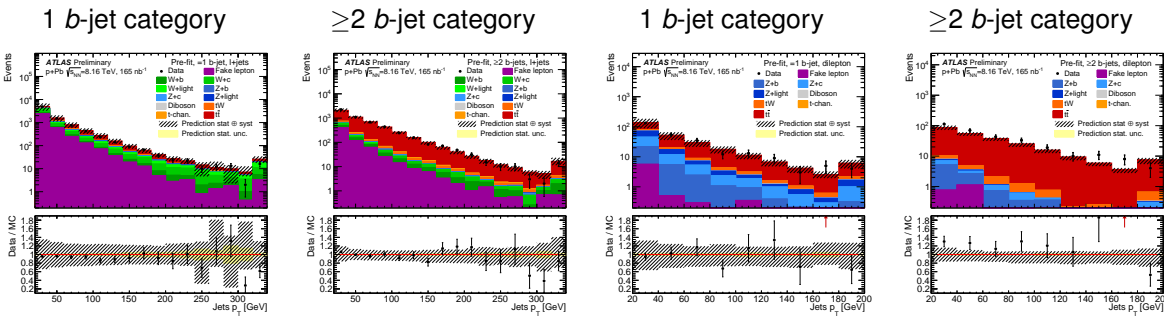
JETM-2023-001



Jet reconstruction

ATLAS-CONF-2023-063

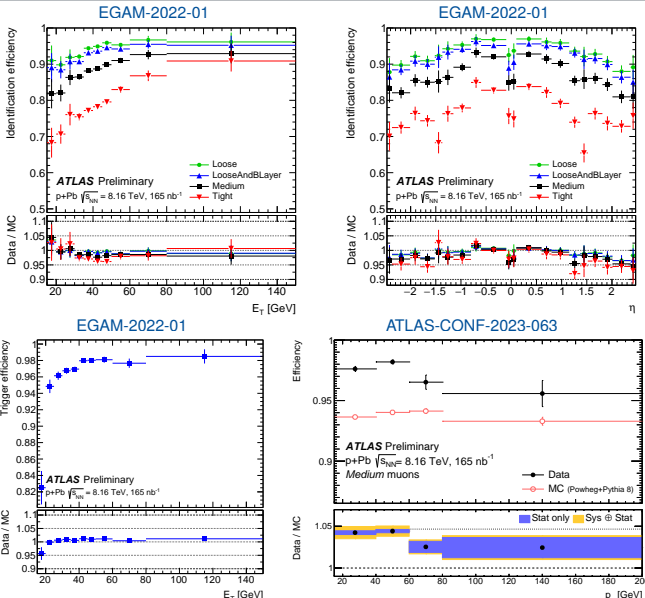
$\ell + \text{jets}$ channel



- ❖ PF jets with b -hadrons are tagged using a recurrent neural network algorithm - DL1 ([EPJ C 79 \(2019\) 970](#)).
- ❖ A good agreement between data and prediction within combined statistical (yellow band) and systematic (hatched band) uncertainties.

Lepton reconstruction

- ❖ Electrons must have $p_T > 18 \text{ GeV}$ and $|\eta| < 2.47$, pass Medium identification and be isolated.
- ❖ Muons must have $p_T > 18 \text{ GeV}$ and $|\eta| < 2.5$, pass Medium requirements and be isolated.
- ❖ Low-pileup egamma calibration and dedicated electron and muon scale factors are applied ([EGAM-2022-01](#)).

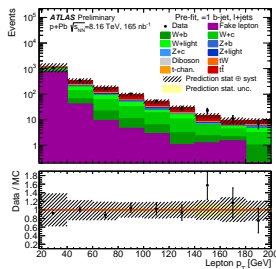


Lepton reconstruction

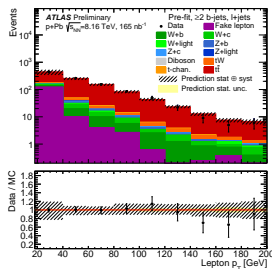
ATLAS-CONF-2023-063

$\ell + \text{jets}$ channel

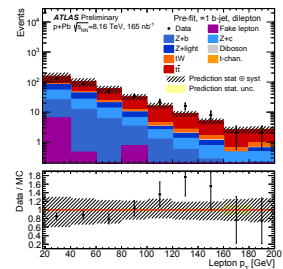
1 b -jet category



≥ 2 b -jet category

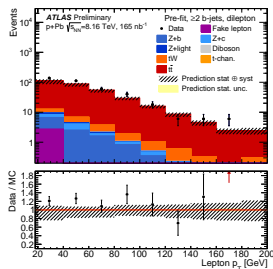


1 b -jet category



Dilepton channel

≥ 2 b -jet category

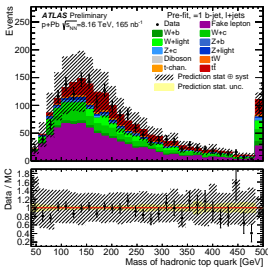
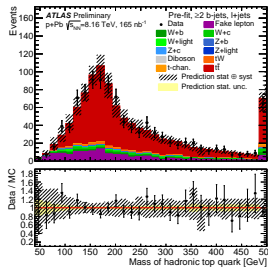


- ❖ Fake lepton background is estimated from data using the matrix-method technique ([arXiv:2211.16178](https://arxiv.org/abs/2211.16178)).
- ❖ A good agreement between data and prediction within combined statistical (yellow band) and systematic (hatched band) uncertainties.

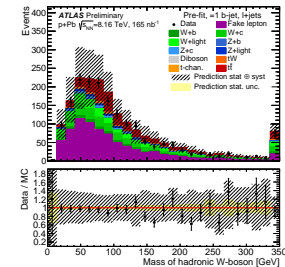
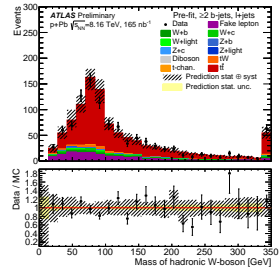
Top quark and W boson

ATLAS-CONF-2023-063

Hadronically decaying top quark

1 b -jet category ≥ 2 b -jet category

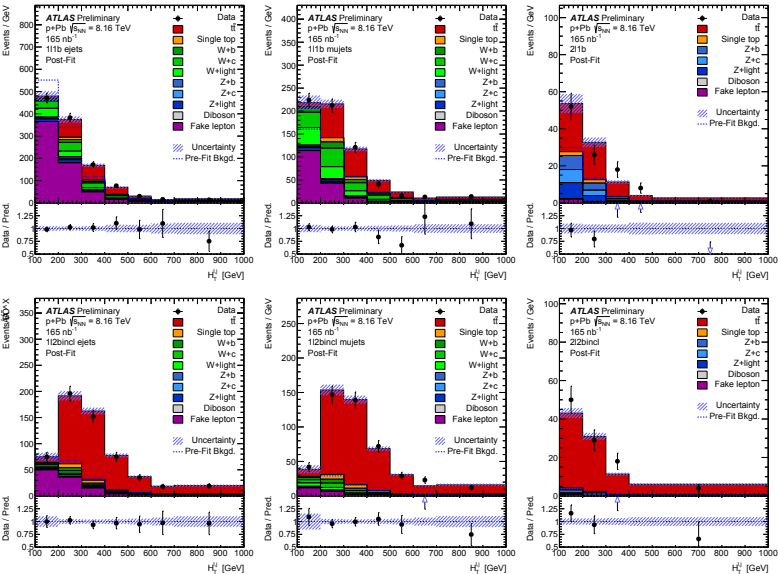
Hadronically decaying W boson

1 b -jet category ≥ 2 b -jet category

- ❖ Invariant mass distributions of hadronically decaying top quark and W boson have been studied in 1 and ≥ 2 b -jet categories.
- ❖ A good agreement is observed between data and prediction within statistical and systematic uncertainties.

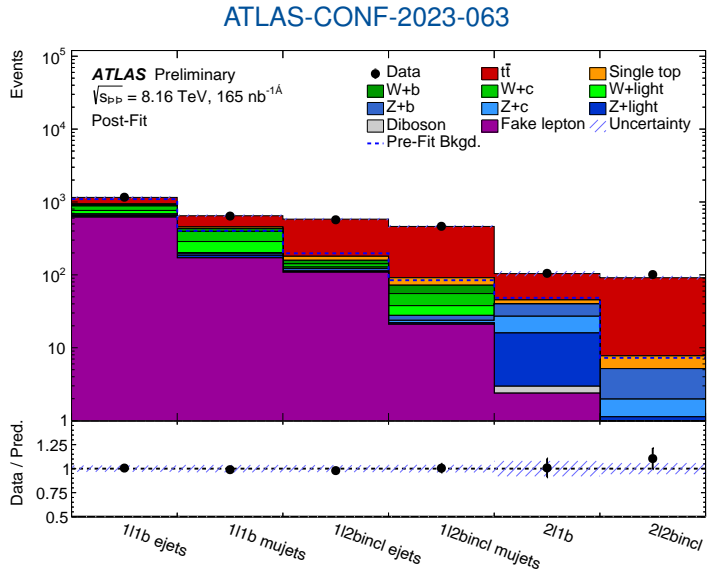
Signal regions

- ❖ Six signal regions are defined using $H_T^{\ell,j}$ distributions.
- ❖ $H_T^{\ell,j}$ is the scalar sum of all lepton and jet p_T .
- ❖ Six signal regions:
 - $4j1b1\ell$ ejets,
 - $4j2binc1\ell$ ejets,
 - $4j1b1\ell$ mujets,
 - $4j2binc1\ell$ mujets,
 - $2j1b2\ell$,
 - $2j2binc12\ell$.



Fitting procedure

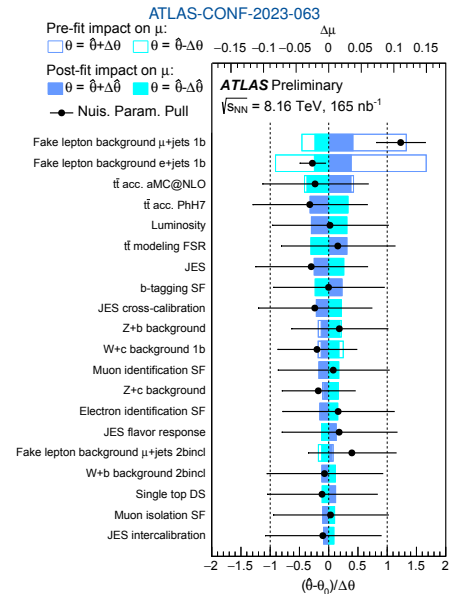
- ❖ The **signal strength** is defined as $\mu_{t\bar{t}} = \sigma_{t\bar{t}}^{\text{measured}} / \sigma_{t\bar{t}}^{\text{theory}}$
- ❖ $\mu_{t\bar{t}}$ is determined using a profile-likelihood method with $H_T^{\ell,j}$ data distributions.
- ❖ The most signal events are found in the $\ell+\text{jets}$ regions with ≥ 2 b -jets.
- ❖ The dilepton channel with ≥ 2 b -jets forms the cleanest signal region.



Systematic uncertainties

- ❖ Systematic uncertainties arise from the lepton and jet reconstruction, b -tagging, fake-lepton background, the signal and background modeling, and luminosity.
- ❖ The main systematic uncertainties include **jet energy scale** and **signal modelling**.
- ❖ The total systematic uncertainty amounts to **9%**.

| Source | unc. up | unc. down |
|------------------------------|---------|-----------|
| Jet energy scale | +0.048 | -0.044 |
| $t\bar{t}$ generator | +0.048 | -0.043 |
| Fake-lepton background | +0.030 | -0.027 |
| Background | +0.030 | -0.025 |
| Luminosity | +0.029 | -0.025 |
| Muon systs. | +0.024 | -0.021 |
| $W+jets$ | +0.023 | -0.020 |
| b -tagging | +0.022 | -0.021 |
| Electron systs. | +0.018 | -0.017 |
| MC statistical uncertainties | +0.011 | -0.010 |
| Jet energy resolution | +0.005 | -0.004 |
| $t\bar{t}$ PDF | +0.001 | -0.001 |
| Total syst. | +0.088 | -0.081 |



Correlations

- ❖ Correlations between all systematic components have been studied.
- ❖ Components with $\geq 30\%$ correlations are presented in a form of the correlation matrix.
- ❖ The largest **correlation** of $\sim 70\%$ is found between fake-lepton background estimation in $e+jets$ and $\mu+jets$ channels.
- ❖ The largest **anticorrelation** of $\sim -75\%$ is observed between fake-lepton background estimation and matching two jet definitions heavy-ion (HI) and particle-flow (PF).

ATLAS Preliminary

ATLAS-CONF-2023-063

| | Fake lepton background e+jets 1b | Fake lepton background e+jets 2bind | Fake lepton background $\mu+jets$ 1b | Fake lepton background $\mu+jets$ 2bind | HI to PF jet matching | W+c-jets background | W+light-jets background | Z+b-jets background | Z+c-jets background | Z+light-jets background | t̄t acc. PhH7 | t̄t acc. aMC@NLO | t̄t shape aMC@NLO | t̄t h _{shape} shape | μ_d | |
|---|----------------------------------|-------------------------------------|--------------------------------------|---|-----------------------|---------------------|-------------------------|---------------------|---------------------|-------------------------|---------------|------------------|-------------------|------------------------------|---------|--|
| Fake lepton background e+jets 1b | 100.0 | 62.2 | 72.0 | 91.4 | -75.4 | -8.5 | 19.4 | 3.9 | 5.2 | -2.7 | -1.2 | 5.7 | 4.6 | 2.1 | 24.1 | |
| Fake lepton background e+jets 2bind | 62.2 | 100.0 | 42.6 | 96.3 | -74.5 | 0.3 | 8.0 | -0.3 | 9.3 | 6.5 | -3.4 | -4.3 | 2.3 | 1.5 | 4.5 | |
| Fake lepton background $\mu+jets$ 1b | 72.0 | 42.6 | 100.0 | 22.9 | -50.5 | -8.3 | -45.4 | 1.1 | 2.6 | 0.2 | -0.9 | 14.0 | -1.2 | 0.9 | 27.9 | |
| Fake lepton background $\mu+jets$ 2bind | 31.4 | 36.3 | 22.9 | 100.0 | -37.3 | -0.7 | 5.8 | -0.6 | 4.3 | 2.2 | -0.4 | -1.6 | -4.4 | 1.2 | 5.9 | |
| HI to PF jet matching | -75.4 | -74.5 | -50.5 | 37.3 | 100.0 | 4.1 | -10.6 | -5.9 | -9.2 | -6.2 | 0.1 | 5.9 | -13.4 | -0.6 | -4.8 | |
| W+c-jets background | -8.5 | 0.3 | -8.3 | -0.7 | 4.1 | 100.0 | -32.1 | 2.4 | 4.3 | 1.6 | 0.1 | -23.9 | -4.6 | -0.0 | -16.6 | |
| W+light-jets background | -19.4 | 8.0 | -45.4 | 5.8 | -10.6 | -32.1 | 100.0 | 1.2 | 3.7 | 1.5 | 0.5 | -4.3 | -0.1 | 1.1 | 2.5 | |
| Z+b-jets background | 3.9 | -0.3 | 1.1 | -0.6 | -5.9 | 2.4 | 1.2 | 100.0 | -41.5 | -9.5 | 5.9 | -1.0 | -2.4 | -0.2 | -13.4 | |
| Z+c-jets background | 5.2 | 9.3 | 2.6 | 4.3 | -9.2 | 4.3 | 3.7 | -41.5 | 100.0 | -38.7 | 11.3 | -13.6 | -3.5 | -0.1 | -16.5 | |
| Z+light-jets background | -2.7 | 6.5 | 0.2 | 2.2 | -6.2 | 1.6 | 1.5 | -9.5 | -38.7 | 100.0 | 1.7 | -2.1 | -1.5 | -0.2 | 3.7 | |
| t̄t acc. PhH7 | -1.2 | -3.4 | -0.9 | -0.4 | 0.1 | 0.1 | 0.5 | 5.9 | 11.3 | 1.7 | 100.0 | -1.1 | -0.6 | -0.1 | -31.7 | |
| t̄t acc. aMC@NLO | 5.7 | -4.3 | 14.0 | -1.6 | 5.9 | -23.9 | -4.3 | -1.0 | -13.6 | -2.1 | -1.1 | 100.0 | 2.4 | 1.8 | 36.8 | |
| t̄t shape aMC@NLO | 4.6 | 2.3 | -1.2 | -4.4 | -13.4 | -4.6 | -0.1 | -2.4 | -3.5 | -1.5 | -0.6 | 2.4 | 100.0 | 30.5 | 1.3 | |
| t̄t h _{shape} shape | 2.1 | 1.5 | 0.9 | 1.2 | -0.6 | -0.0 | 1.1 | -0.2 | -0.1 | -0.2 | -0.1 | 1.8 | 30.5 | 100.0 | 4.7 | |
| μ_d | 24.1 | 4.5 | 27.9 | 5.9 | -4.8 | -16.6 | 2.5 | -13.4 | -16.5 | 3.7 | -31.7 | 36.8 | 1.3 | 4.7 | 100.0 | |

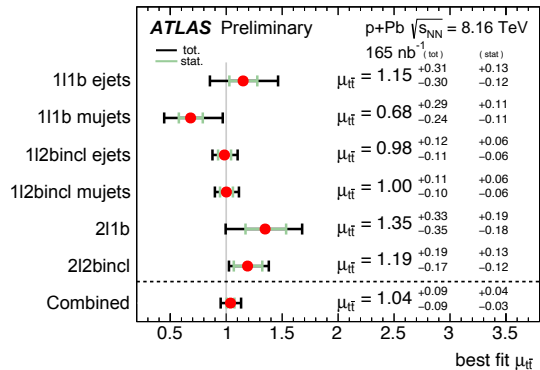
Cross-section measurement

- ❖ The top-quark pair production cross section is measured to be

$$\sigma_{t\bar{t}} = 57.9 \pm 2.0 \text{ (stat.)} {}^{+4.9}_{-4.5} \text{ (syst.) nb.}$$

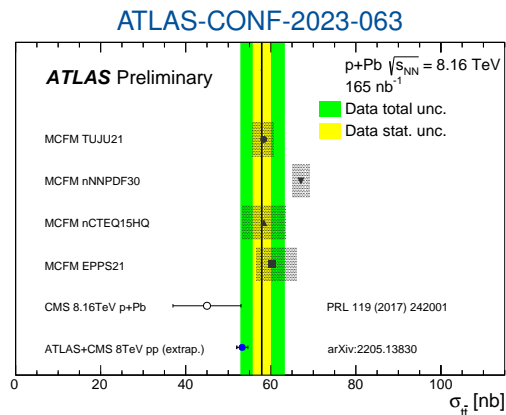
- ❖ The total uncertainty amounts to **9%**, which makes it the most precise $t\bar{t}$ measurement in HI collisions.
- ❖ The significance is well over **5σ** in the ℓ +jets and dilepton channels separately.
- ❖ First observation of top-quark pair production in the **dilepton channel** in $p+Pb$ collisions.

ATLAS-CONF-2023-063

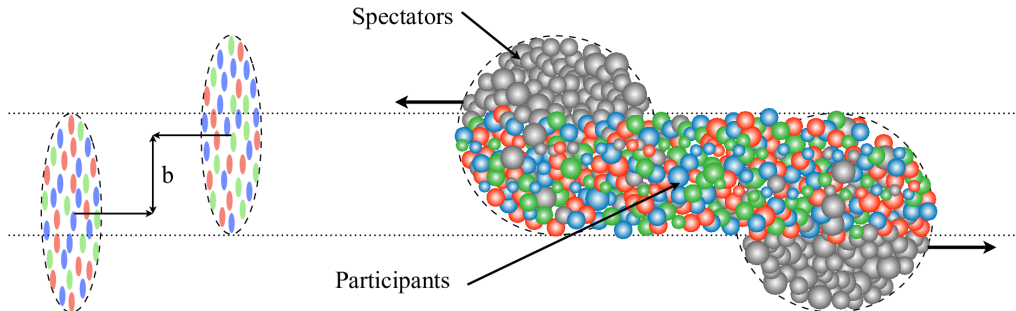


Comparison to other experimental results and theory

- ❖ The cross section is compared to the **CMS measurement** in the $p\text{+Pb}$ system.
- ❖ The result is consistent with the cross section in **pp collisions**, scaled by $A = 208$ and extrapolated to $\sqrt{s} = 8.16 \text{ TeV}$.
- ❖ The measured $t\bar{t}$ cross section is compared to the **MCFM NNLO calculation** ([PRD 94, 093009 \(2016\)](#)) for four nPDF sets.
 - The largest deviation is observed for the nNNPDF3.0 set with 2σ significance.
 - A good agreement is found with NNLO calculation based on other nPDF sets.



Prospects of $t\bar{t}$ in Pb+Pb



- ❖ Pb+Pb data collected by ATLAS:
 - **Run 2:** 1.4 nb^{-1} at $\sqrt{s_{\text{NN}}} = 5.02 \text{ TeV}$ in 2018,
 - **Run 3:** 1.7 nb^{-1} at $\sqrt{s_{\text{NN}}} = 5.36 \text{ TeV}$ in 2023.
- ❖ Centrality varies from ultra-peripheral \rightarrow peripheral \rightarrow central,
top quarks are expected to be produced with higher probability in central collisions.

CMS Pb+Pb measurement

- ❖ First evidence of $t\bar{t}$ production in dilepton final states in heavy-ion collisions in CMS.

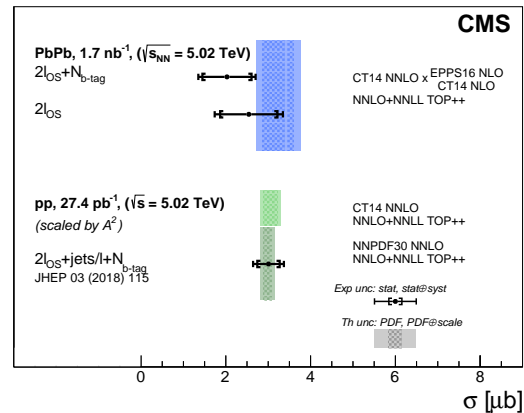
- ❖ Total integrated luminosity of **1.7 nb⁻¹**.

- ❖ Measurement uses a fit to Boosted Decision Tree discriminator distributions.

- ❖ Observed significance:
3.8 σ (dilepton-only),
4.0 σ (dilepton + b -jets).

- ❖ Measured cross sections for two methods:
 $\sigma_{t\bar{t}} = 2.54^{+0.84}_{-0.74} \mu\text{b}$ (dilepton-only),
 $\sigma_{t\bar{t}} = 2.03^{+0.71}_{-0.64} \mu\text{b}$ (dilepton + b -jets).

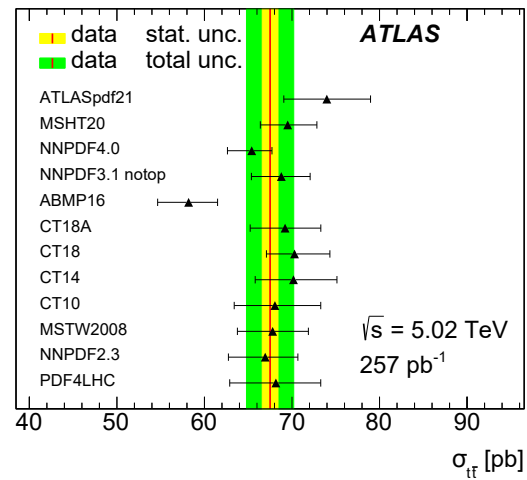
PRL 125 (2020), 222001



ATLAS pp 5.02 TeV measurement

- ❖ pp at $\sqrt{s} = 5.02$ TeV represents a reference system to Pb+Pb collisions at the same energy.
- ❖ Total integrated luminosity of **257 pb⁻¹**.
- ❖ Measurement combines $\ell + \text{jets}$ and dilepton decay modes.
- ❖ Very precise $t\bar{t}$ cross-section measurement:
 $\sigma_{t\bar{t}} = 67.5 \pm 0.9 \text{ (stat.)} \pm 2.3 \text{ (syst.)}$
 $\pm 1.1 \text{ (lumi.)} \pm 0.2 \text{ (beam) pb.}$
- ❖ $pp \sigma_{t\bar{t}}$ scaled by A^2 can be compared to Pb+Pb $\sigma_{t\bar{t}}$.

JHEP 06 (2023) 138



Summary

- 1 The top-quark pair production cross section has been measured to be

$$\sigma_{t\bar{t}} = 57.9 \pm 2.0 \text{ (stat.)} {}^{+4.9}_{-4.5} \text{ (syst.) nb.}$$

- 2 The significance is well over 5σ in the dilepton channel, resulting in the first observation of $t\bar{t}$ production in the dilepton channel in $p+\text{Pb}$ collisions.
- 3 The result is consistent with the CMS measurement, the scaled cross section in pp collisions and NNLO calculation based on four nPDF sets.
- 4 A combination with the CMS measurement could further improve $t\bar{t}$ cross-section precision in $p+\text{Pb}$ collisions.
- 5 A $t\bar{t}$ measurement in $\text{Pb}+\text{Pb}$ collisions by ATLAS is also envisaged.

Acknowledgements

Research project partly supported by the National Science Centre of Poland under grant number UMO-2020/37/B/ST2/01043 and by PL-GRID infrastructure.

